2013 IEEE/RSJ International Conference on
Intelligent Robots and Systems (IROS)
November 3-7, 2013. Tokyo, Japan

VNSA: Variable Negative Stiffness Actuation based on Nonlinear Deflection Characteristics of Buckling Beams

Mustafa Yalcin, Bircan Uzunoglu, Elif Altintepe and Volkan Patoglu

***Abstract*— We present variable negative stiffness actuation (VNSA), an alternative method of achieving variable stiffness actuation based on the nonlinear deflection characteristics of buckling beams. The approach exploits transverse stiffness variations of axially loaded beams around their critical buckling load to achieve an actuator with adjustable stiffness. In particular, transverse stiffness of buckled beams are positive under tensile loading and for compressive loading below their first critical buckling load, while they display *negative* stiffness above this critical value. Furthermore, for small deflections transverse stiffness of buckled beams depends linearly on the amount of axial loading. Consequently, the stiffness of a variable stiffness actuator can be modulated (i) by decreasing the transverse stiffness through an increase of the axial compressive loading on a beam, up to values above the first critical buckling load where the overall stiffness of the actuator approaches its lowest negative value, and (ii) by increasing the transverse stiffness through application of tensile axial loading. Capitalizing on the concept of negative stiffness, the lowest stiffness of VNSA can be set arbitrarily close to zero or even to negative values (when counterbalanced), while very high stiffness values are also achievable by tensile loading of the beam. As a result, VNSA can modulate its stiffness over a uniquely large range that includes zero and negative stiffness values. Furthermore, thanks to the negative stiffness characteristics, the stiffness of VNSA can be kept very low without sacrificing the mechanical integrity and load bearing capacity of the actuator. We introduce the design of VNSA, theoretically analyze its stiffness modulation response, and provide implementation details of a prototype. We also provide experimental results detailing range of stiffness modulation and force tracking performance achieved with this prototype and discuss its correspondence with the theory.**

I. INTRODUCTION

Emerging technologies and increased use of robots to aid daily activities have emphasized the safety of humans while interacting with robots. Safe human-machine interactions are possible with backdriveable robot designs. Although backdriveability can be achieved by designing light-weight robots with direct drive actuation and low friction power transmission, such robots cannot withstand high forces/torques due to actuator saturation. In applications where large forces/torques are required, backdriveability of the robots can be made possible by active force control. Unfortunately, such active systems are vulnerable to power losses. Moreover, since force sensors possess very high stiffness, after an impact with the environment, force controlled robots may behave unexpectedly, possibly injuring a human operator. An alternative way to achieve safe physical interactions between robots and humans when large forces/torques are necessitated is to deliberately introduce compliant elements to the design. Compliance adds a level of back-drivability by decreasing the end-effector impedance and filters impulsive disturbances, while allowing high forces/torques be rendered via active feedback control within the control bandwidth.

While adding compliance to an actuator, different levels of stiffness are required for various interactions: Precise position control tasks with good disturbance rejection characteristics require actuators with high stiffness, while interaction forces and impulsive loads can be better regulated using actuators with low stiffness. Consequently, variable stiffness actuators (VSAs) have been introduced to allow for selection of most proper impedance during a task. VSAs are special type of compliant mechanisms that feature adjustable stiffness via controlled "spring like" elements. In this study, we propose a novel variable stiffness actuator design based on the concept of negative stiffness.

In the literature, three major approaches have been proposed to control stiffness of VSAs [1]: (i) antagonistic-control, (ii) mechanical control, and (iii) structure-control. The antagonistic-control approach to design of variable stiffness actuators is inspired from human muscles. In antagonistic VSAs, two motors are connected to "spring like" compliant elements, while these compliant elements are connected to the output link. The opposing movement of the two actuators creates compression forces on one element and tension on the other. It has been shown in literature that if the the springs possess non-linear force-deflection characteristics (e.g., if they are quadratic), these conjugate actuator movements do not affect the configuration of the output link position, but changes its stiffness under quasi-static conditions [2]. Similarly, if both actuators move in the same direction, the configuration of the output link is changed, while preserving its stiffness.

Implementation of variable stiffness actuators with the antagonistic-control approach has been studied by several research groups. For instance, in [3] Bicchi *et al.* proposed a VSA actuator based on McKibben artificial muscles and further developed it in [4]. In [5], Migliore *et al.* introduced use of curved surfaces to create nonlinear spring elements. In [6], Yamaguchi *et al.* implemented antagonistic joints for biped locomotion, while bidirectional antagonistic joints were utilized by DLR in [7].

Mechanical-control approach modules effective stiffness by varying the points where the compliant element is attached to the system, that is, by changing the pre-load of the elastic element. In one implementation, VSA consists of

This work has been partially supported by TUBITAK Grant 111M186.
M. Yalcin, B. Uzunoglu, E. Altintepe and V. Patoglu are with Faculty of Engineering and Natural Sciences, Sabancı University, Istanbul, Turkey. {myalcin,bircanuzun,ealtintepe,vpatoglu}@sabanciuniv.edu

three bodies and an actuator controls the position between the actuated and fixed bodies. A spring is attached from the actuated body to a third auxiliary frame and it is loaded or flexed by a second actuator. Compared to antagonistic-control based designs, this approach is easier to build, since the compliant elements are allowed to have linear stiffness and only a single spring is sufficient to change the effective stiffness of the actuator. This design is also advantageous with respect to antagonist approach since it allows more flexibility in the actuator selection. A well known actuator design based on the mechanical-control approach is the MACCEPA actuator [8]. This design has been shown to be the more energy efficient compared to antagonistic designs [9]. Another mechanical-control approach detailed in [10] and [11] modulates stiffness by changing the pivot point of a lever arm attached to the compliant element. With such a design, stiffness can be modulated over a large interval, ranging from zero to structural stiffness of the device. Other VSAs based on this approach include [12], [13].

In the structure-control approach, variations in stiffness is achieved through manipulation of the effective structure of the spring. In this approach, stiffness and position adjustments are mechanically separated, such that one actuator controls the stiffness, while the other one controls the position of the joint. Generally, actuators that control the position need to be more powerful than the actuators that change stiffness, as a result selecting the proper actuator for the specific task may decrease the power consumption. Another advantage of separating the stiffness and position actuators is that, the footprint of the mechanism may be decreased since the link can be driven directly; however, this approach may introduce nonlinearities to the actuator reponse [2], [9].

Several designs have emerged following the structure-control idea. For instance, in [14] and [15] rotated leaf springs are used for stiffness modulation. In particular, in these designs the aspect ratio of a bending beam; hence, its stiffness, is modulated by rotating the beam. In [16], moment of inertia of a bending beam is changed using a layered beam structure. To increase stiffness, new layers are introduced to the bending beam. In [17] effective length of a bending beam is controlled to modulate stiffness, while in [18] active coils of a helical spring are controlled.

In this study, we present an alternative method of achieving variable stiffness actuation based on the nonlinear buckling behavior of axially loaded beams: variable negative stiffness actuation (VNSA). This new mechanical-control approach exploits the transverse stiffness variation of axially loaded beams around their first critical buckling load to achieve an actuator with adjustable stiffness. In particular, transverse stiffness of buckled beams are positive for tensile loading and compressive loading below first critical buckling load, while they possess *negative* stiffness above this critical buckling load. Moreover, transverse stiffness depends linearly on the amount of axial loading for small deflections. Consequently, the stiffness of VNSA can be modulated (i) by decreasing the transverse stiffness through an increase of the axial compressive loading on a beam, up to values above the first critical buckling load where the overall stiffness of the actuator approaches its lowest negative value, and (ii) by increasing the transverse stiffness through application of tensile axial loading.

The proposed approach of stiffness modulation is advantageous, since capitalizing on the concept of negative stiffness, the lowest stiffness of VNSA can be set arbitrarily close to zero or even to negative values, while high stiffness values are also achievable through tensile loading of the beam. As a result, VNSA can modulate its stiffness over a large range that also includes negative stiffness values. Furthermore, thanks to the negative stiffness characteristics, the stiffness of VNSA can be kept low without sacrificing the mechanical integrity and load bearing capacity of the actuator.

Negative stiffness of VNSA can be utilized in design of exoskeletons and prosthetic devices. For instance, one can capitalize on actuators with negative stiffness to assist walking during parts of the gait cycle. Negative stiffness may also be used to significantly decrease the overall coupled impedance during physical human robot interaction.

II. Transverse Stiffness of Buckling Beams under Axial Loading

Extreme stiffness systems due to negative stiffness elements have received some attention in the literature [19], [20]. Negative stiffness systems are also employed in several applications, for instance as vibration isolators [21]–[23], bistable compliant mechanisms [24]–[26] and constant-force mechanisms [27]. Similar to these works, we also utilize negative transverse stiffness of buckling beams, but different from these studies, we use negative stiffness for modulation of VSA compliance.

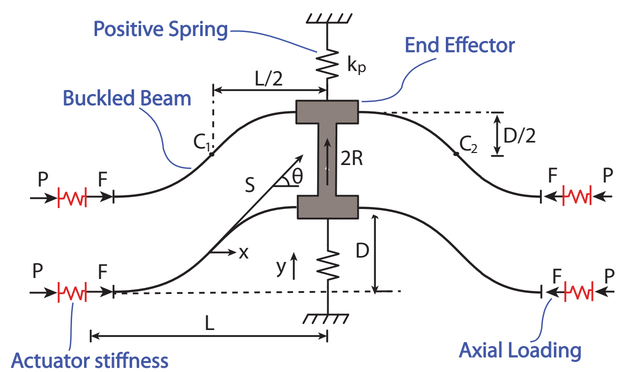

Fig. 1. Schematic model of axially loaded buckling beam system coupled to compression springs

Figure 1 presents a schematic model of axially loaded buckling beams coupled to compression linear springs k_p. In the figure, clamped-clamped the boundary conditions for the beams are depicted, while it is possible to conduct similar analysis for other boundary conditions. Moreover, the deflection pattern is valid only for small deflections and for axial loadings that are well below the second critical buckling load. Let L denote half of axial length of the beam, where D signifies its transverse deflection. Axial loading is represented with P, while the transverse loading is given as $2R$. Since actuator stiffness K has been represented red colored spring like elements, effective force loads beams are depicted as F. The path length along the deflected beam is measured using the variable s. Symbol x denotes axial direction, while y axis lies along the transverse direction. In Figure 1, C_1 and C_2 mark the inflection points and the boundary conditions for analysis can be taken as $y(0) = 0$ and $y(L/4) = D/2$. Following analysis closely follows the one presented in [24].

Noting the following curvature relationship

$$\frac{d\theta}{ds} = \frac{1}{\sqrt{1-y'^2}}.y'' \tag{1}$$

and considering the moment induced by the axial and transverse loads P and $2R$ on an infinitesimal beam element located between C_1 and C_2, one can invoke the moment curvature relationship from solid mechanics as

$$\frac{-Py - Rx}{EI} = \frac{d\theta}{ds} = \frac{y''}{\sqrt{1-y'^2}} \tag{2}$$

where E is the modulus of elasticity and I is the area moment of inertia of the beam.

Let $x(s)$ represent the horizontal projection of s onto x axis

$$x(s) = \int_0^s \sqrt{1-y'^2}ds \tag{3}$$

For small deflections of the beam satisfying $|y'| << 1$, Eqn. (2) can be approximated as

$$-Py - R\int_0^s (1 - \frac{y'^2}{2})ds = EIy''\Big(1 + \frac{y'^2}{2}\Big) \tag{4}$$

To proceed further, an assumption should be introduced characterizing the shape of the beam under axial loading. For axial loadings that are below the second critical buckling load, the shape of the buckling beam between inflection points C_1 and C_2 can be closely approximated by a perfect sinusoid [24]. To introduce sinusoidal mode shape assumption to the analysis, let

$$y(s) = A\sin(ws) \tag{5}$$

where $w = \frac{2\pi}{L}$, $A = \frac{D}{2}$ and $D_1 = \frac{D}{2}$. Introducing Eqn. (5) and its derivatives into Eqn. (4) and collecting terms one can express that

$$-PD_1\sin(ws) - R\Big(s - 0.25D_1^2w^2s - 0.125D_1^2 w\sin(2ws)\Big) = -EID_1w^2\sin(ws)\Big(1 + \frac{D_1^2w^2}{2}\cos^2(ws)\Big) + R(D_1, s) \tag{6}$$

where $R(D_1, s)$ is the error function defined as

$$R(D_1, s) = -PD_1\sin(ws) - Rs + 0.25RD_1^2w^2s + 0.125RD_1^2w\sin(2ws) + EID_1w^2 sin(ws)\Big(1+\frac{D_1^2w^2}{2}\cos^2(ws)\Big) \tag{7}$$

After applying method of weighted residuals in the Galerkin form of

$$\int_0^{L/4} \sin(ws)R(D_1, s)ds = 0 \tag{8}$$

left hand side of the equation can be explicitly stated as

$$-\frac{1}{8}D_1P\Big(L - \frac{2\sin(\frac{Lw}{2})}{w}\Big) - R\frac{\sin(\frac{Lw}{4}) - \frac{1}{4}Lw\cos(\frac{Lw}{4})}{w^2} - \frac{1}{4}D_1^2Rw^2\frac{\sin(\frac{Lw}{4}) - \frac{1}{4}Lw\cos(\frac{Lw}{4})}{w^2} + \frac{1}{8}D_1^2Rw\frac{2\sin^3(\frac{Lw}{4})}{3w} + \frac{1}{8}EID_1w^2\Big(L - \frac{2\sin(\frac{Lw}{2})}{w}\Big) + \frac{1}{64}EID_1^3w^4(L - \frac{\sin(Lw)}{w}) = 0 \tag{9}$$

Noting that $w = \frac{2\pi}{L}$, normalizing the equation by P_{cr} and L^2 to obtain $\frac{D_1}{L}$ and $\frac{P}{P_{cr}}$ instead of D_1 and P, where $P_{cr} = \frac{4\pi^2 EI}{L^2}$ is the first critical axial load for a clamped-clamped end points configuration, one can obtain

$$-\frac{1}{8}(\frac{P}{P_{cr}})(\frac{D_1}{L}) - \frac{1}{4\pi^2}(\frac{R}{P_{cr}}) + \frac{1}{3}(\frac{R}{P_{cr}})(\frac{D_1}{L})^2 + \frac{1}{8}(\frac{D_1}{L}) + \frac{1}{16}\pi^2(\frac{D_1}{L})^3 = 0 \tag{10}$$

Hence, the algebraic relation between the transverse displacement D_1 of a beam subjected to an axial loading P and the transverse force $2R$ acting on it can be expressed as

$$\frac{P}{P_{cr}}(\frac{D_1}{L}) + \frac{R}{P_{cr}}\Big[\frac{2}{\pi^2} - \frac{8}{3}(\frac{D_1}{L})^2\Big] = \frac{D_1}{L}\Big[1 + \frac{\pi^2}{2}(\frac{D_1}{L})^2\Big] \tag{11}$$

To relate axial loading to transverse stiffness, denote the actuator/transmission stiffness along the axial direction as K and the force exerted by the actuator as F, then axial loading can be expressed as [24]

$$P = F - K(\delta_e + \delta_b) \tag{12}$$

where δ_e is axial deflection of the axially loaded beam due to its elasticity and δ_b signifies the axial deflection caused due to buckling of the beam. Residual stresses are neglected in our analysis, since their effect on axial force is very limited for large scale devices such as ours. Noting that the axial stiffness of the beam is given as AE/L, where A is the cross sectional area of the beam, $P = AE\delta_e/L$. So, the axial load applied to deflecting beam spring can be formulated as

$$P = (F - K\delta_b)\Big(\frac{AE/L}{K + AE/L}\Big) \tag{13}$$

Introducing the dimensionless variables $\xi = D/2L$ and $\gamma = K/(AE/L)$, invoking small deflection assumption stating $\xi << 1$, Eqns. (11) and (13) can be solved together to reveal

$$\frac{2R}{P_{cr}} = -K_{b1}\xi + K_{b3}\xi^3 \tag{14}$$

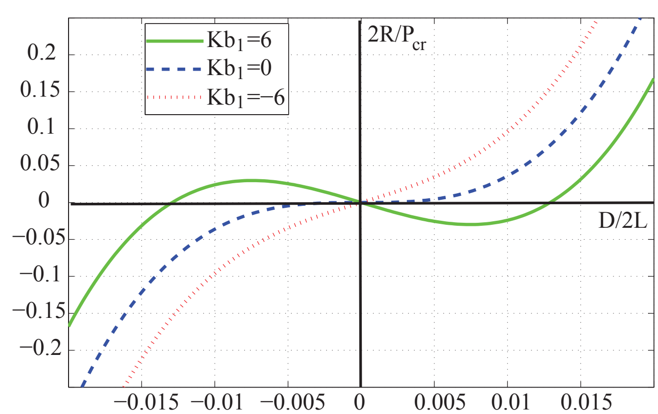

Fig. 2. Non-dimensionalized transverse load vs. displacement plot for a clamped-clamped beam under axial loading. The slope of the curves signify transverse stiffness.

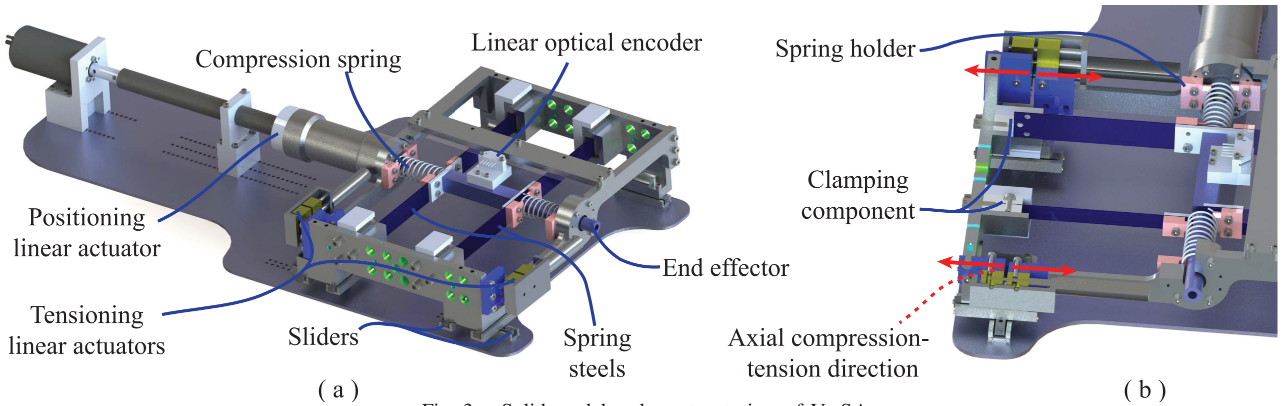

Fig. 3. Solid model and a cut-out view of VNSA

where K_{b1} and K_{b3} are linear and cubic spring constants for the beam under axial loading P. In this equation, the linear and cubic spring constants are given as

$$K_{b1} = \Big(\frac{F}{P_{cr}(1+\gamma)} - 1\Big)\pi^2 \tag{15}$$

$$K_{b3} = \bigg(\Big(\frac{AE\gamma}{P_{cr}(1+\gamma)} - \frac{4}{3}\Big(\frac{F}{P_{cr}(1+\gamma)} - 1\Big)\Big)\bigg)\pi^4 \tag{16}$$

Figure 2 depicts the nondimensionalized transverse load curves according to Eqn. (14). According to Eqn. (15) K_{b1} changes proportional to axial force F exerted by linear actuator. As depicted at Figure 2, for different values of axial loading, positive, zero and negative stiffness can be obtained. In particular, when the compression force applied to beam exceeds the first critical bucking load (case $K_{b1} > 0$ in Figure 2) buckling takes place and negative stiffness behavior of the beam can be observed. Moreover, for tensile axial loading (case $K_{b1} < 0$), the beam possesses positive transverse stiffness values that increase as the tension increases.

III. Design of VNSA

Solid model of VNSA is presented in Figure 3(a). VNSA consists of a two actuation modules: one for positioning of the actuator and another for axial loading of the beams used for stiffness modulation. Positioning module is responsible for linear movement of the moving frame. A close-up of tensioning module is presented also in Figure 3(b). This module adjusts the transverse stiffness of leaf springs by changing axial compressive or tensile forces acting on the spring steel. In order to ensure uniform axial loading without inducing moments on the leaf springs, two tensioning actuators are attached to moving base in a symmetrical manner. Linear sliders are used to support transverse movements of the moving base and to guide axial movements of the tensioning mechanism.

Two leaf springs are responsible for generating adjustable (negative) stiffness coefficients and these springs are attached to the moving base with clamped-clamped boundary conditions. End-effector is clamped to the center of leaf springs and the tip of end-effector is extended with a custom designed shaft to allow interactions with the environment. One or two (positive) compression springs are attached to the leaf springs in parallel to set the nominal stiffness of VNSA to a desired value. Transverse deflection of end-effector with respect to the moving base is measured with a linear optical encoder, as marked in Figure 3(a).

IV. Implementation of VNSA

Figure 4 presents a functional prototype of VNSA. In this implementation, the positioning module consists of a linear screw drive actuator with 0.5" lead. Linear actuator is driven by a 90 W graphite brushed DC motor equipped with a 4.8:1 planetary gear head and 2000 counts per revolution[1] optical encoder. The positioning module possesses high friction and is non-backdriveable. The end-effector of positioning module is attached to the moving base of VNSA. The moving base is composed of the end-effector, tensioning module and the leaf springs. Precision low friction sliders with 2" stroke are attached at bottom of the moving base to support the weight of mechanism.

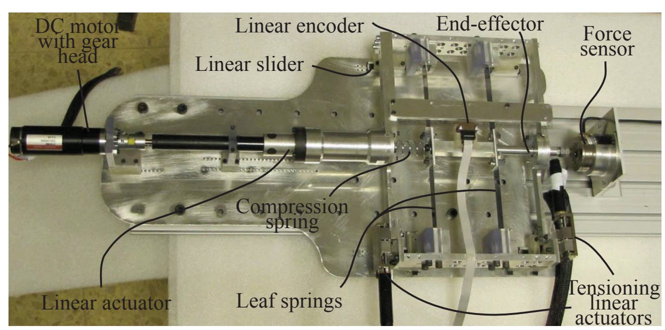

Fig. 4. Prototype of VNSA

Two high tensile blue tempered (AISI 1095) steel sheets with 0.254 mm thickness and 20 mm width are used as the buckling beams. One steel compression spring with 1.239 N/mm stiffness is attached between end-effector and moving base of the mechanism. Deflection of the end-effector with respect to moving base, that is, deflection of leaf spring and compression spring attached to end-effector, is measured by 2000 counts per inch linear optical encoder.

The tensioning module consists of two linear micro precision actuators connected to the moving base. Two 3.5 W DC motors with 64 counts per revolution optical encoders and

[1] Encoder counts are given under quadrature decoding.

84:1 planetary gear heads are used for actuating the reciprocating slides of the tensioning modules. Reciprocating slides are placed on 0.03" inch lead screws. Since the lead screws are non-backdriveable, no actuation is necessary to maintain a desired level of compression/tension. Tensioning modules are supported with four low friction precision sliders, as a result friction losses and hysteresis are low for the axially loaded beams.

The end-effector of VNSA consists of custom made aluminum and rapid-prototyped clamping components, as well as the leaf springs. The effective mass of end-effector is kept below 100 grams.

V. EXPERIMENTAL CHARACTERIZATION OF VNSA

Figure 5 presents experimental data collected for transverse forces and deflections of VNSA under different tensile axial loads. During experiments, a force sensor with 0.01 N precision is attached in front of the end-effector in order to measure transverse forces applied by VNSA. As predicted by the theoretical model in Section II, as axial tension on the leaf springs is increased, higher positive stiffness values are observed. Moreover, the stiffness is dominated by the linear stiffness coefficient K_{b1} of Eqn. (14), while effect of the cubic stiffness coefficient K_{b3} vanishes under tensile loading. Model predicted values of transverse forces/deflections matches the experimental data very closely and are not depicted not to clutter Figure 5.

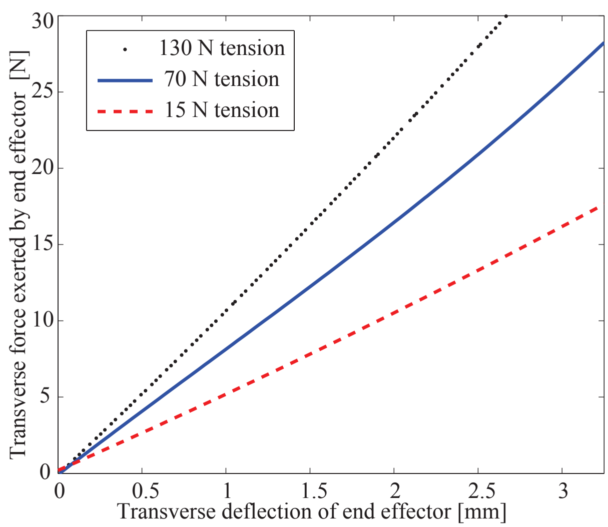

Fig. 5. Stiffness change of VNSA under axial tensile loading

Figure 6 presents experimental data collected for transverse forces and deflections of VNSA under different compressive axial loads. In order to clearly demonstrate negative stiffness effect taking place during buckling and post-buckling, positive stiffness of the compression spring is subtracted from the data presented this figure. Experimental results indicate that, as expected, the stiffness of VNSA decreases under compressive loading of leaf springs. The transverse stiffness of leaf springs reaches zero at the critical buckling load of 53.2 N and negative stiffness values can observed for post-buckling compressive loads. Unlike the tensile loading case, the transverse force/deflection plots becomes highly nonlinear as the transverse deflection increases, since the effect of cubic stiffness coefficient K_{b3} dominates the force response for large deflections. Nevertheless, the linear stiffness coefficient K_{b1} still determines the transverse stiffness of leaf springs under small deflections. As a consequence, the axially loaded leaf springs act as negative linear springs for small deflections.

In these experiments, modulation of stiffness of VNSA is achieved by position control of the linear tensioning actuators. In particular, required axial deflection to impose desired level of the tensile or compressive axial force on the beam is estimated based on the axial stiffness of the beam and its traverse deflection using the theoretical model presented in Section II, Eqn. (14). Then, linear tensioning actuators are regulated to this value under closed loop position control.

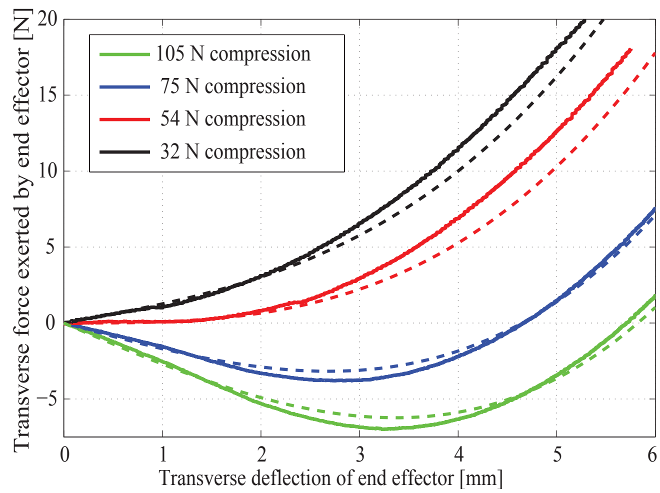

Fig. 6. Stiffness change of VNSA under axial compression. Experimental data is plotted together with model predicted values indicated as solid lines.

In Figure 6, model predicted values of transverse forces/deflections (indicated with dashed lines) are plotted together with the experimental data for comparison. The agreement between the theoretical estimates and the experimental data is quite good for small transverse deflections, where the linear stiffness coefficient K_{b1} dominates. As the effect of the cubic stiffness coefficient K_{b3} becomes large enough, the quality of the match decreases. One of the important reasons for the mismatch is the effect of non-characterized actuator/transmission stiffness K along the axial direction, which plays an important role in the determination of K_{b3}. Deviation for the small deflection assumption is another error source for model based predictions.

Figure 7 presents force tracking performance of VNSA under different levels of stiffness values. During these force tracking experiments, a force sensor is attached to ground in front of end-effector of VNSA to validate its measurements. Force tracking performance under explicit force control for high (5 N/mm), medium (3 N/mm) and low (1 N/mm) end-effector stiffness values are plotted in Figure 7. For the high stiffness value, the force tracking performance is low. This result is expected, since due to non-collocation

TABLE I

EXPERIMENTAL CHARACTERIZATION OF VNSA AT MAX. AND MIN. STIFFNESS VALUES

Criteria	Stiffness [N/mm]	Stroke [mm]	Force Resolution [N]	Backdriveability [N]	Stored Energy
Max. Stiffness	12.5	7	0.15875	3 (at 1 Hz) - 10 (at 0.2 Hz)	0.0064 Joule
Min. Stiffness	-5	2	0.000127	0.8 (at 1 Hz) – 2.5 (at 0.2 Hz)	0.3215 Joule

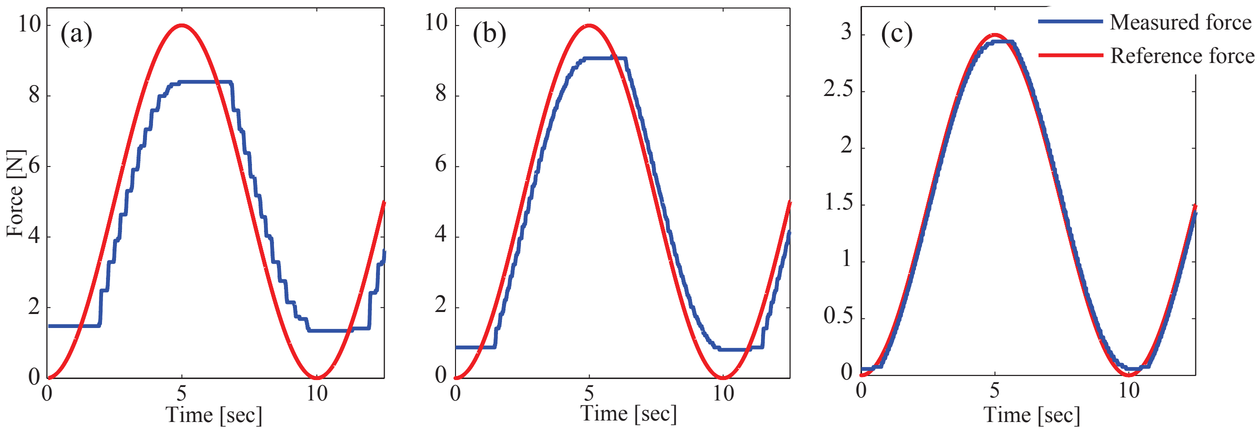

Fig. 7. Force tracking performance of VNSA under (a) high (5 N/mm), (b) medium (3 N/mm) and (c) low (1 N/mm) stiffness settings.

between actuation and force sensing unit, high stiffness in the force measurement introduces a low upper limit for the control gains. Without high control gains, the stick-slip friction in the lead screw and the planetary gear head cannot be robustly compensated and the force tracking performance stays low. As the mechanical stiffness of VNSA is decreased to 3 N/mm, higher control gains can be implemented, and better force tracking performance has been obtained. Finally, when the mechanical stiffness is decreased to 1 N/mm, which requires the leaf springs to have negative transverse stiffness values, high control gains can be implemented without sacrificing stability. As a result, stick-slip effects are compensated by the controller and high fidelity force tracking performance is achieved for a system driven by a lead screw attached to a planetary gear head.

Table I lists experimental characterization results for the active backdriveability for VNSA under its maximum and minimum stiffness settings. Minimum stiffness of VNSA can be set arbitrarily close to zero and can even be made negative if the end effector is counter balanced by an external positive spring. Maximum and minimum stiffness of VNSA is observed as 12.5 N/mm and -5 N/mm and these limits are determined by the force bearing capacity of the tensioning module used for this particular implementation. Given its nominal stiffness set as 1.5 N/mm (by the positive compression spring), VNSA can increase its stiffness almost one order of magnitude. Backdriveability of VNSA is determined by the position controller gains and the actuator bandwidth. As stiffness decreases, force resolution increases for a given optical encoder. Backdriveability also increases since larger controller gains can be used to compensate for disturbances.

The potential energy stored within the axially loaded beams around first buckling loads can be calculated by integrating Eqn. (14) along the transverse deflection D. The maximum energy that can be stored for the current prototype is calculated as 0.3215 J.

The transverse deflection range of VNSA where the stiffness coefficient behaves linearly is dependent on the amount of axial loading. For our current prototype, tensile loading of leaf springs, VNSA stiffness behaves linearly for transverse deflections up to 7 mm, while linear stiffness is bound to transverse deflections of 2 mm for low stiffness settings under compressive axial loads. However, since the nonlinear stiffness of VNSA can be characterized, this stiffening stiffness model can be used for control of the device, for instance as in [28], when larger forces/deflections are necessitated.

VI. CONCLUSION AND FUTURE WORKS

An alternative method of achieving variable stiffness actuation based on the nonlinear deflection characteristics of buckling beams (VNSA) has been introduced. A working prototype of the concept proposed and implemented. Feasibility tests have been conducted and the efficiency of the device in terms of modulating stiffness and achieving good force tracking performance has been demonstrated.

The transverse deflection range of current prototype is relatively low, especially for the linear stiffness range under compressive axial loads. This does not pose an issue for applications where high energy storage in the device is undesired (e.g. for safety concerns) and high resolution encoders can be utilized. For other applications, larger traverse deflections can be achieved by increasing the length of the buckling beams, that is, by enlarging the footprint for the device. An alternative solution is to utilize a cascaded series design as shown in Figure 8. In such a design, end-effector (center) of each leaf spring is attached to the clamping mechanism of consecutive leaf spring module such that traverse deflection of bucking beams are superimposed. In particular, a mechanical summer may be implemented for the transverse deflections of multiple beams.

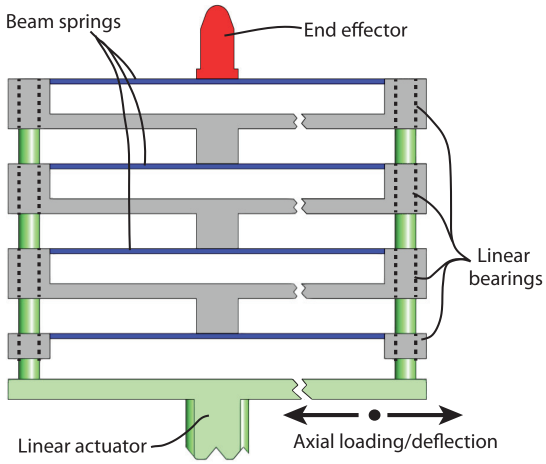

Fig. 8. Cascaded Series Design ofVNSA

Note that bistable beams are commonly used in MEMS structures; hence, miniaturization of VNSA concept is feasible. For example, a micro-scale series elastic actuator [29], [30] with very low stiffness can be implemented utilizing the negative stiffness of buckling beams. Moreover, piezoelectric actuators can be employed for high-bandwidth stiffness modulation. It is also possible to implement the buckling beams and tensioning module as a monolitic structure. Utilizing compliant linear fixtures as linear guides, such a design can eliminate friction losses of the current linear slides and virtually eliminate hysteresis.

REFERENCES

[1] R. Ham, T. Sugar, B. Vanderborght, K. Hollander, and D. Lefeber, "Compliant actuator designs," *IEEE Robotics Automation Magazine*, vol. 16, no. 3, pp. 81–94, 2009.

[2] C. English and D. Russell, "Mechanics and stiffness limitations of a variable stiffness actuator for use in prosthetic limbs," *Mechanism and Machine Theory*, vol. 34, no. 1, pp. 7–25, 1999.

[3] A. Bicchi and G. Tonietti, "Fast and "soft-arm" tactics [robot arm design]," *IEEE Robotics Automation Magazine*, vol. 11, no. 2, pp. 22–33, 2004.

[4] R. Schiavi, G. Grioli, S. Sen, and A. Bicchi, "VSA-II: A novel prototype of variable stiffness actuator for safe and performing robots interacting with humans," in *IEEE International Conference on Robotics and Automation*, 2008, pp. 2171 –2176.

[5] S. A. Migliore, E. A. Brown, and S. P. DeWeerth, "Novel nonlinear elastic actuators for passively controlling robotic joint compliance," *Journal of Mechanical Design*, vol. 129, no. 4, pp. 406–412, 2007.

[6] J. Yamaguchi, D. Nishino, and A. Takanishi, "Realization of dynamic biped walking varying joint stiffness using antagonistic driven joints," in *IEEE International Conference on Robotics and Automation*, vol. 3, 1998, pp. 2022–2029.

[7] F. Petit, M. Chalon, W. Friedl, M. Grebenstein, A. Schaffer, and G. Hirzinger, "Bidirectional antagonistic variable stiffness actuation: Analysis, design and implementation," in *IEEE International Conference on Robotics and Automation*, 2010, pp. 4189–4196.

[8] R. Ham, T. Sugar, B. Vanderborght, K. Hollander, and D. Lefeber, "Compliant actuator designs," *IEEE Robotics Automation Magazine*, vol. 16, no. 3, pp. 81–94, 2009.

[9] B. Vanderborght, R. Van Ham, D. Lefeber, T. G. Sugar, and K. W. Hollander, "Comparison of Mechanical Design and Energy Consumption of Adaptable, Passive-compliant Actuators," *The International Journal of Robotics Research*, vol. 28, no. 1, pp. 90–103, 2009.

[10] A. Jafari, N. G. Tsagarakis, B. Vanderborght, and D. Caldwell, "A novel actuator with adjustable stiffness (AwAS)," in *IEEE/RSJ International Conference on Intelligent Robots and Systems*, 2010.

[11] A. Jafari, N. G. Tsagarakis, and D. Caldwell, "AwAS-II: A new actuator with adjustable stiffness based on the novel principle of adaptable pivot point and variable lever ratio," in *IEEE International Conference on Robotics and Automation*, 2011.

[12] S. Wolf and G. Hirzinger, "A new variable stiffness design: Matching requirements of the next robot generation," in *IEEE International Conference on Robotics and Automation*, 2008.

[13] L. Visser, R. Carloni, and S. Stramigioli, "Variable stiffness actuators: A port-based analysis and a comparison of energy efficiency," in *IEEE International Conference on Robotics and Automation*, 2010, pp. 3279–3284.

[14] K. Hollander and T. Sugar, "Concepts for compliant actuation in wearable robotic systems," in *US-Korea Conf. Science, Technology and Entrepreneurship*, 2004, pp. 644–650.

[15] H. Seki, A. Takada, Y. Kamiya, M. Hikizu, and H. Nomura, "Development of a robot joint mechanism with variable compliance by rotating a leaf spring," in *Japan/USA Flexible Automation Conference*, 2000, pp. 13 019–13 024.

[16] S. Kawamura, T. Yamamoto, D. Ishida, T. Ogata, Y. Nakayama, O. Tabata, and S. Sugiyama, "Development of passive elements with variable mechanical impedance for wearable robots," in *IEEE International Conference on Robotics and Automation*, 2002.

[17] T. Morita and S. Sugano, "Development of a new robot joint using a mechanical impedance adjuster," in *IEEE International Conference on Robotics and Automation*, 1995, pp. 2469–2475.

[18] K. Hollander, T. Sugar, and D. Herring, "Adjustable robotic tendon using a Jack Spring," in *IEEE International Conference on Rehabilitation Robotics*, 2005, pp. 113–118.

[19] R. Lakes, T. Lee, and Y. Wang, "Extreme stiffness systems due to negative stiffness elements," *Nature*, vol. 410, pp. 565–567, 2001.

[20] Y. Wang and R. Lakes, "Extreme stiffness systems due to negative stiffness elements," *American Journal of Physics*, vol. 72, no. 1, pp. 40–51, 2004.

[21] D. L. Platus, "Negative stiffness mechanism vibration isolation systems," in *Vibration Control in Microelectronics, Optics, and Metrology*, 1992.

[22] J. E. John, "A discussion of zero spring rate mechanisms used for the active isolation mount experiment," National Aeronautics and Space Administration, Tech. Rep., 11 1999.

[23] L. Zhaochun, W. Xiaojie, B. Majid, M. Nicholas, and G. Faramarz, "A tunable 'negative' stiffness system for vibration control," in *Active and Passive Smart Structures and Integrated Systems*, 2012.

[24] M. Taher and A. Saif, "On tunable bistable mems - theory and experiment," *Journal of Microelectromechanical Systems*, vol. 9, no. 2, pp. 158–170, 2000.

[25] P. Cazottes, A. Fernandes, J. Pouget, and M. Hafez, "Bistable buckled beam: Modeling of actuating force and experimental validations," *Journal of Mechanical Design*, vol. 131, 2009.

[26] G. L. Holst, G. H. Teichert, and B. D. Jensen, "Modeling and experiments of buckling modes and deflection of fixed-guided beams in compliant mechanisms," *Journal of Mechanical Design*, vol. 133, no. 5, 2011.

[27] Y. Chen and C. Lan, "An adjustable constant-force mechanism for adaptive end-effector operations," *ASME Journal of Mechanical Design*, vol. 134, no. 3, pp. 031 005–1–9, 2012.

[28] H. Yu, S. Huang, N. V. Thakor, G. Chen, S. L. Toh, Y. Ghorbel, M. S. Gruz, and C. Zhu, "A novel compact compliant actuator design for rehabilitation robots," in *IEEE International Conference on Rehabilitation Robotics*, 2013.

[29] O. Tokatli and V. Patoglu, "Optimal design of a micro series elastic actuator," in *ASME International Design Engineering Technical Conferences*, 2010.

[30] ——, "Series elastic actuation for force controlled micromanipulation," in *IEEE International Conference on Mechatronics*, 2011.